

# Simulation of single-phase flow past cylinder

Manideep Roy<sup>#1</sup>, Sagar Debnath<sup>#2</sup>

<sup>#1</sup>Mechanical Engineering Department, National Institute of Technology, Durgapur  
Mahatma Gandhi Avenue, Durgapur, West Bengal, India-713209

## Abstract

The objective is to analyse the flow physics in flow past cylinders for sub critical flow regime in the present study. The software used is Fluent 17.1. It is found that pressure decreases, and turbulent kinetic energy suddenly increases the cylinder's flow downstream. Flow separation and wake effects can be visualized. The Fast Fourier Transform (FFT) is also done using MATLAB software, which indicates multiple frequencies in drag and lifts forces.

**Keywords** — FFT, Flow separation, turbulent kinetic energy, subcritical

## I. INTRODUCTION

### A. Venturi-meter

A venturi-meter is a device used to measure the flow rate of a fluid flowing through a pipe. The fluid may be a liquid or a gas. The main parts of a venturi-meter are a short converging part, throat, and a diverging part. Venturi-meter is based on the principle of Bernoulli's Equation. Inside the pipe, the pressure difference is created by reducing the cross-sectional area of the flow passage. This pressure difference is measured with a manometer's help and helps determine the rate of fluid flow or other discharge from the pipeline.

### B. Flow past Cylinder

Flow past a circular cylinder usually experiences boundary layer separation and very strong flow oscillations in the body's wake region. In a certain Reynolds number range, a periodic flow motion will develop in the wake due to the boundary layer being shed alternatively from either side of the cylinder. This regular pattern of vortices in the wake is called a Karman vortex street. It creates an oscillating flow at a discrete frequency correlated to the Reynolds number of the flow. The periodic nature of the vortex shedding phenomenon can sometimes lead to unwanted structural vibrations, especially when the shedding frequency matches one of the structure's resonant frequencies.

## II. LITERATURE REVIEW

Mishra and Peles [1] experimentally investigated hydrodynamic cavitation in micro ventures using microfabrication and high-speed photography. They observed flow patterns such as traveling bubble

cavitation and supercavitation. They found that single supergravity was formed, which extends up to the microchannel exit. Moreover, there was no evidence of flow rate choking.

Cioncolini *et al.* [2] experimentally investigated choked cavitation with three circular micro-orifices with diameters of 150  $\mu\text{m}$  and 300  $\mu\text{m}$  and thicknesses of 1.04 mm, 1.06 mm, and 1.93 mm. They found that the cavitation number at the inception and cessation of choked cavitation increases with an increase in the micro-orifice diameter and thickness but was independent of the upstream pressure, downstream pressure, average flow velocity, and orifice Reynolds number. At choking, the upstream pressure ratio to the downstream pressure is constant for a given micro-orifice. In contrast, during the choked flow, the micro-orifice's mass flow rate is proportional to the upstream pressure's square root.

Iben *et al.* [6] analyzed the gas release inflow behind the orifice using optical methods. They detected the number and size of the bubbles through a detection algorithm based on Hough Transformation. It was observed that the number and size of the gas bubbles increase with the increasing pressure difference.

Mishra and Peles [4] investigated cavitation inflow through a micro-orifice inside a silicon microchannel using microfabrication techniques. They found that the low incipient cavitation number suggests a dominant size scale effect, and choking cavitation was observed to be independent of any pressure or velocity scale effects. Large flow and cavitation hysteresis were detected at the microscale leading to very high desinent cavitation numbers.

## III. GEOMETRIES INVESTIGATED

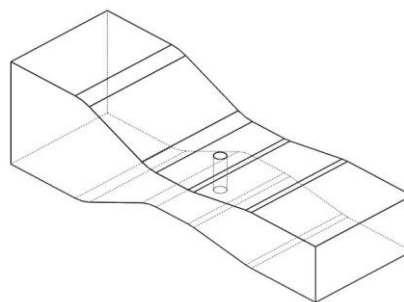


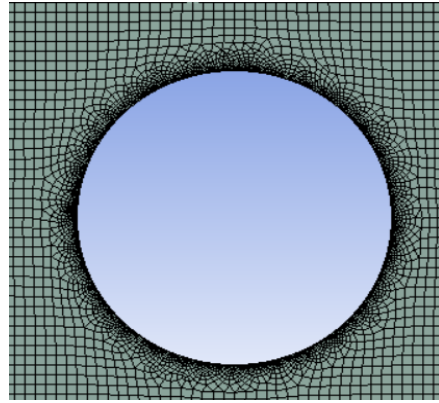
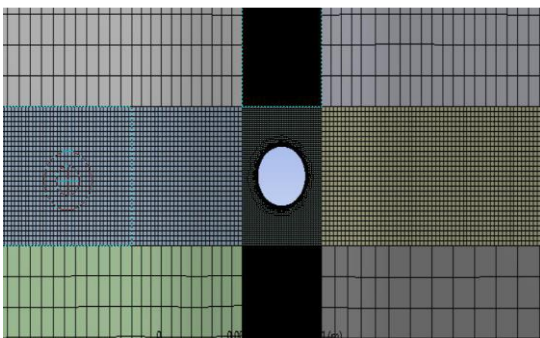
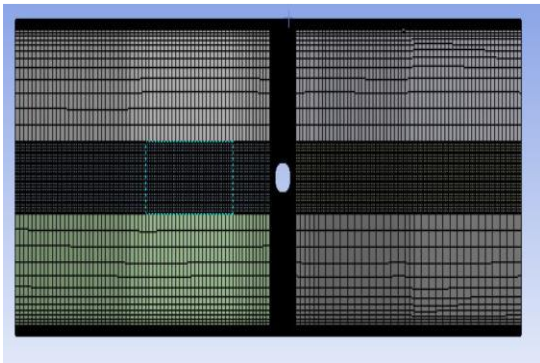
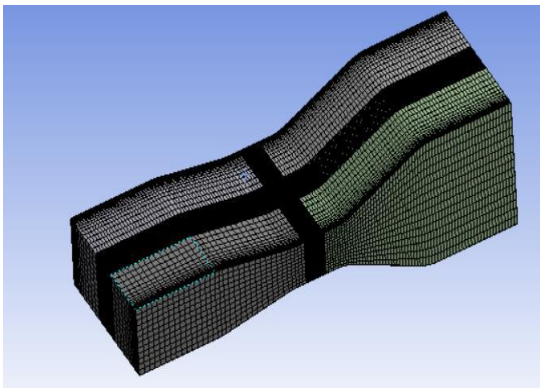
Fig. 1 3D venturi meter with a cylinder at the throat.



Figure 1 shows the computational domain with the following specifications:

- Throat diameter = 10 mm
- Upstream diameter = 30 mm
- Total Convergence angle = 52 degree
- Total Divergence angle = 20 degree
- Length of the throat = 10 mm
- Inlet Velocity = 6m/sec
- Depth = 30 mm
- The diameter of the cylinder = 3 mm, ensuring a blockage ratio of 10%

#### IV. MESHING



**Fig. 2 Computational mesh showing finer mesh near the cylinder and coarser mesh away from the cylinder.**

3D Structured meshing is done using ANSYS ICEM CFD software, as shown in Figure 2. Finer meshing is done across the cylinder and at the walls to maintain the  $y^+$  value. The total number of nodes and elements of the half geometry are 2129905 and 2009527, respectively. The mesh's minimum orthogonal quality is 4.16284e-01, the maximum orthogonal skew is 4.03825e-01, and the maximum aspect ratio is 2.44520e+02.

#### V. BOUNDARY CONDITIONS

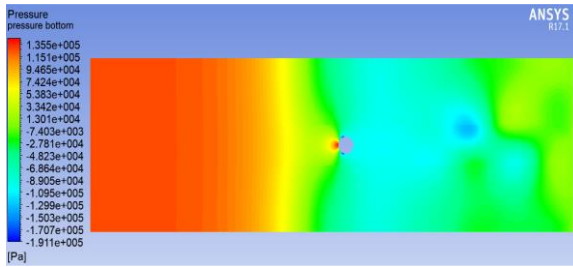
Inlet velocity is taken as 6m/sec. Atmospheric pressure is specified at the outlet. No-slip boundary conditions are specified at the walls. Simulation is done using half geometry to reduce the computation time. So, the symmetric boundary condition is specified.

#### VI. SOLUTION SCHEME

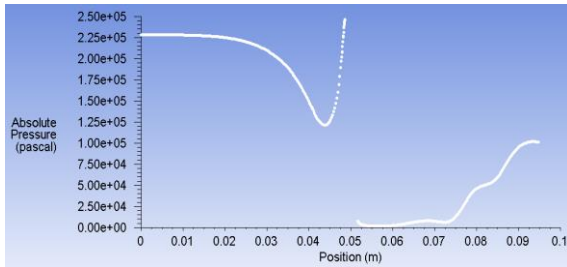
First, the simulation was run using the steady-state solver. They are using this as the initial condition transient simulation was applied. The simulation started with the first order discretization scheme, but after a few steps, the second order upwind discretization scheme is employed for pressure and momentum to obtain higher accuracy. Pressure-velocity coupling has been done using the SIMPLE algorithm. Residuals have been continuously monitored for continuity, x velocity, y velocity, k, and omega. The convergence criteria for all the residuals are set to  $10^{-5}$ . SST  $k-\omega$  turbulent model is used because it combines both the  $k-\epsilon$  and  $k-\omega$  turbulent model.  $k-\omega$  turbulent model is used to get an accurate solution in the near-wall boundary region, whereas the  $k-\epsilon$  turbulent model is used away from the wall. The time step size was set to 0.0001 based on the Strouhal number and Nyquist criterion. Convergence is achieved at each and every time step.

**VII. RESULT AND DISCUSSION**

**A. Pressure Variation**



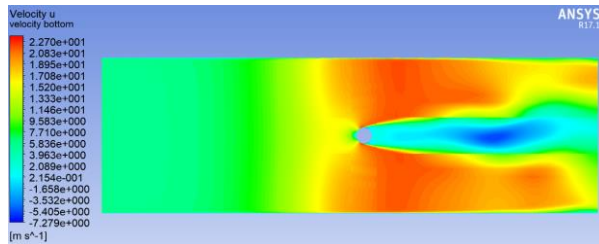
**Fig. 3 Pressure Variation at the transverse midplane of the venturi meter.**



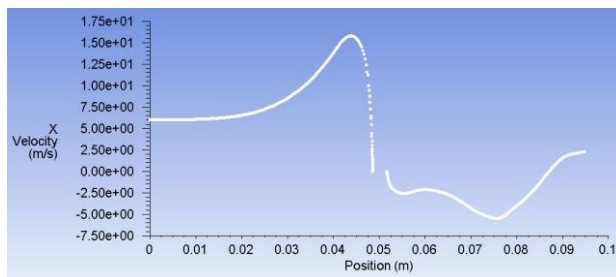
**Fig. 4 Variation of absolute pressure versus position along the venturi meter's transverse midplane centerline.**

Fig. 3 and 4 indicate a discontinuity in the pressure variation near the cylinder at the throat. Pressure decreases abruptly the downstream of the flow after the cylinder. If the local pressure decreases below the liquid's vapor pressure, the formation of cavities will occur.

**B. Velocity Variation**



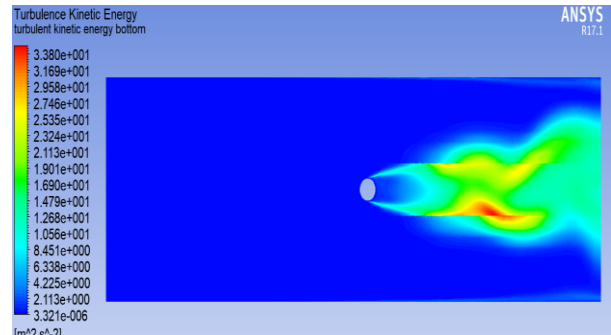
**Fig. 5 Longitudinal velocity variation at the transverse midplane of the venturi meter.**



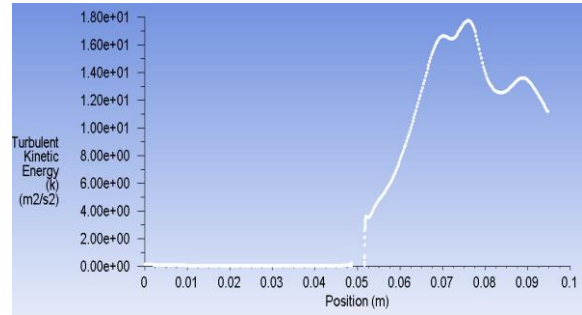
**Fig. 6 Variation of longitudinal velocity versus position along the venturi meter's transverse midplane centerline.**

Fig 5 and 6 indicates that velocity increases rapidly at the throat and then suddenly decreases. The negative value of velocity indicates flow separation. From the velocity contour, the wake effect can be visualized.

**C. Turbulent Kinetic Energy**



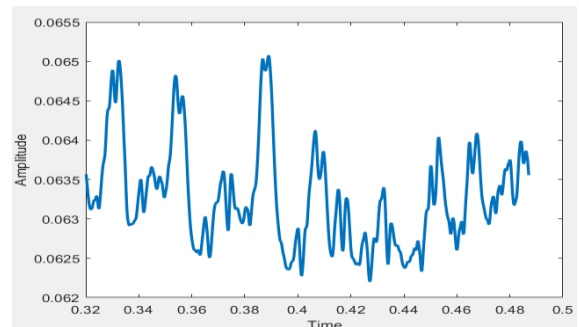
**Fig. 7 Contour of Turbulent Kinetic Energy at the transverse midplane of the venturi meter.**



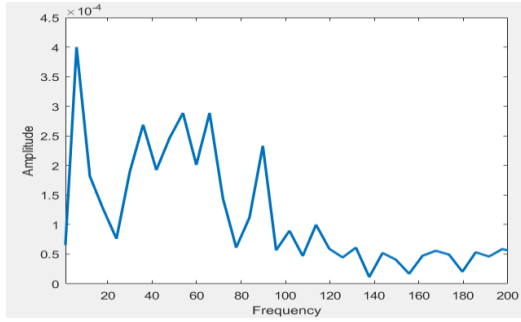
**Fig. 8 Variation of longitudinal velocity versus position along the venturi meter's transverse midplane centerline.**

Fig 7 and 8 indicate that turbulent kinetic energy increases rapidly downstream of the flow after the cylinder. Turbulent kinetic energy is maximum where the collapsing of the bubbles take place. When the cavities collapse, a huge amount of energy is generated.

**D. Fast Fourier Transform**



**Fig. 9 Plot of drag versus time**



**Fig. 10 Fluctuations in drag versus frequency using FFT (Fast Fourier Transform) in MATLAB.**

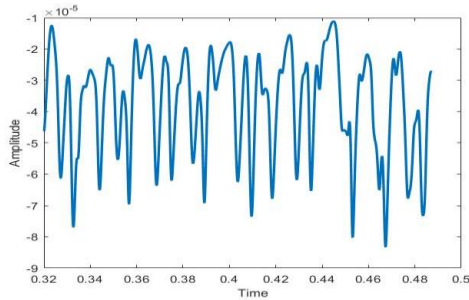


**Fig. 11 Plot of lift versus time**

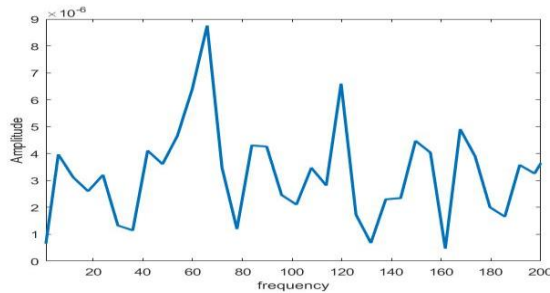


**Fig 12. Fluctuations in lift versus frequency using FFT in MATLAB.**

Fig 9-12 indicates the presence of multiple frequencies in the drag and lift. The maximum

amplitude of drag is obtained at a frequency of 6 Hz, whereas the maximum amplitude of lift is obtained at around 60 Hz.

### VIII. CONCLUSION

Pressure decreases, and turbulent kinetic energy increases the downstream of the flow after the cylinder. Flow separation is indicated by the negative values of longitudinal velocity. The wake effect is also visualized using velocity and turbulent kinetic energy contour. Moreover, the Fast Fourier Transform of drag and lift indicates the presence of multiple frequencies.

### ACKNOWLEDGMENT

I want to thank 'Sagar Debnath' of the National Institute of Technology Durgapur for helping me out in doing this project.

### REFERENCES

- [1] C. Mishra, Y. Peles, An experimental investigation of hydrodynamic cavitation in micro-Venturis, *Phys. Fluids* 18 (2006) 103603.
- [2] A. Cioncolini, F. Scenini, J. Duff, M. Szolcek, M. Curioni, Choked cavitation in micro-orifices: An experimental study, *Exp. Therm. Fluid Sci.* 74 (2015) 49-57
- [3] Nidhul K, Sunil A S, Kishore V, Influence of Lateral Boundaries, and Grid Spacing on Steady Flow Past a Square Cylinder, *SSRG-IJME- 1(8)* (2014).
- [4] C. Mishra, Y. Peles, Cavitation inflow through a micro-orifice inside a silicon microchannel, *Phys. Fluids* 17 (2005) 013601.
- [5] Pankaj Kumar, Study of cavitation behind a circular cylinder at upper subcritical flow regime, Ph.D. Thesis, Indian Institute of Technology, Madras, 2016.
- [6] U. Iben, F. Wolf, H. Freudigmann, J. Fröhlich, W. Heller, Optical measurements of gas bubbles in oil behind a cavitating micro-orifice flow, *Exp. Fluids* 56 (2015) 114.